Timescale competition controls tipping behaviour under climate overshoot

Lars Ackermann

lars.ackermann@awi.de

Alfred Wegener Institute for Polar and Marine Research https://orcid.org/0000-0001-6643-0714

Matteo Willeit

Potsdam Institute for Climate Impact Research

Gregor Knorr

Alfred Wegener Institute, Helmholtz Centre for Polar and Marine Research https://orcid.org/0000-0002-8317-5046

Yuchen Sun

https://orcid.org/0000-0002-2449-8718

Uta Krebs-Kanzow

Alfred Wegener Institute, Helmholtz Centre for Polar and Marine Research

Christian Rodehacke

Alfred-Wegener-Institut Helmholtz-Zentrum for Polar und Marine Research https://orcid.org/0000-0003-3110-3857

Gerrit Lohmann

Alfred Wegener Institute https://orcid.org/0000-0003-2089-733X

Physical Sciences - Article

Keywords: Earth System Resilience, Greenland Ice Sheet, Atlantic Overturning Circulation, Future Warming Scenarios

Posted Date: February 27th, 2026

DOI: https://doi.org/10.21203/rs.3.rs-8941071/v1

Additional Declarations: There is **NO** Competing Interest.

Timescale competition controls tipping behaviour under climate overshoot

Lars Ackermann[1*], Matteo Willeit[2†], Gregor Knorr[1†], Yuchen Sun[1†], Uta Krebs-Kanzow[1†], Christian Rodehacke[1,3†], Gerrit Lohmann[1,4†]

[1*]Paleoclimate Dynamics, Alfred Wegener Institute, Helmholtz Centre for Polar and Marine Research, Klussmannstrasse 3, Bremerhaven, 27570, Germany.
[2]Potsdam Institute for Climate Impact Research, P.O. Box 60 12 03, Potsdam, 14412, Germany.
[3]Nationalt Center for Klimaforskning (NCKF), Danish Meteorological Institute, Sankt Kjelds Plads 11, Copenhagen, 2100, Denmark.
[4]Department of Physics, University of Bremen, Otto-Hahn-Allee 1, Bremen, 28359, Germany.

*Corresponding author(s). E-mail(s): lars.ackermann@awi.de;
Contributing authors: matteo.willeit@pik-potsdam.de; gregor.knorr@awi.de; yuchen.sun@awi.de; uta.krebs-kanzow@awi.de; christian.rodehacke@awi.de; gerrit.lohmann@awi.de;
†These authors contributed equally to this work.

Abstract

Tipping elements of the Earth system are often framed as threshold phenomena governed by peak global warming [1–3]. However, climate components operate on widely differing intrinsic timescales [4–6], so the outcome of overshoot warming may depend not only on temperature thresholds but also on the interaction between forcing duration and system inertia.

Here we use a comprehensive Earth system model with interactive ocean circulation, Arctic sea ice and a fully coupled Greenland Ice Sheet to simulate multi-millennial trajectories under extended overshoot scenarios [7]. We find that reversibility is strongly component-specific. Fast components, including the Atlantic Meridional Overturning Circulation (AMOC) and Arctic sea ice, weaken during peak forcing but recover as greenhouse-gas concentrations decline. In

contrast, the Greenland Ice Sheet shows persistent mass loss and long-term commitment even under strong mitigation, consistent with its slow dynamical adjustment and geometry-dependent feedback [8–10]. Despite freshwater fluxes exceeding 0.1 Sv, AMOC collapse does not occur, highlighting the importance of spatial meltwater routing and advective export [11–13].
Our results demonstrate that Earth system reversibility cannot be inferred from peak warming alone. Instead, overshoot duration reorganizes the hierarchy of tipping elements according to intrinsic process timescales. Tipping is therefore a dynamical outcome emerging from timescale competition within a coupled system. These findings imply that even temporary overshoot can irreversibly commit slow structural components of the climate system, redefining how climate stabilization targets should be interpreted on millennial timescales [14, 15].

Keywords: Earth System Resilience, Greenland Ice Sheet, Atlantic Overturning Circulation, Future Warming Scenarios

Main

Despite significant advances in climate modeling, major uncertainties persist regarding the long-term evolution of the Earth system under sustained anthropogenic forcing. Key questions remain about the resilience of critical climate components such as the Greenland Ice Sheet (GrIS) [8, 10, 16], Arctic sea-ice [2, 17–19], and the Atlantic Meridional Overturning Circulation (AMOC) [20–22], and their potential to cross irreversible tipping points within the coming millennia. These uncertainties arise not only from imperfect knowledge of individual processes, but from the intrinsic inertia of the climate system itself. Slow Earth system components like ice sheets and the deep ocean shape future climate trajectories beyond the next centuries. Addressing these uncertainties is essential for refining the concept of planetary boundaries [14] and for informing strategies to mitigate long-term climate risks.

Many studies highlight the risk of tipping cascades in which changes in one Earth system component trigger changes in another [2, 3, 15]. However, tipping behavior depends critically on timescales, which differ by orders of magnitude across climate subsystems. As a result, interactions among slow components are difficult to capture in comprehensive Earth system models (ESMs), and most studies rely on conceptual models or models of intermediate complexity [23].

In particular, polar ice sheets, such as the GrIS, are a decisive element in long-term future projections [19]. However, accounting for the ice sheets' inertia and resolving feedback processes requires multi-millennial simulations with complex ESMs. Although interactive ice sheets are increasingly included in ESMs [24–36], long-term projections with such models remain rare [37]. This limitation is critical for assessing AMOC evolution, which is often studied using idealized freshwater perturbations rather than dynamically evolving meltwater input [11, 12, 21, 38]. Such approaches capture ocean-circulation mechanisms but neglect the spatial and temporal variability of meltwater release. Climate projections from the sixth Coupled Model Intercomparison Project (CMIP6) likewise omit Greenland meltwater fluxes [20–22, 39], yet still

show an AMOC decline, albeit with large uncertainty. Studies that include meltwater effects typically lack interactive ice sheets or sufficient resolution and integration time [26, 31, 32, 35, 40, 41].

Here, we run the state-of-the-art comprehensive AWI Earth System Model (AWI-ESM) to simulate global climate and Greenland ice sheet evolution over the next 2,000 years. The model has been applied for paleoclimate simulations on glacial-interglacial time scales [42, 43], providing a robust framework for our projections. In this study, we explore the resilience and irreversibility of key climate system components over multi-millennial timescales while accounting for the intrinsic inertia of slow climate components and the interplay between ice-sheet dynamics, ocean circulation, and sea-ice evolution.

Reversible components: Arctic sea ice and AMOC

Transient simulations with prescribed atmospheric greenhouse gas concentrations and orbital configurations for four different extended future scenarios (Fig. 1, Tab. A1) are performed with the Earth system model AWI-ESM (see Methods). The modelled historical global mean temperature increase follows observations [44, 45]. In the scenarios, CO_2 peaks between 2100 and 2250 at 610 ppm (SSP2-4.5) and 2,150 ppm (SSP5-8.5) before declining, whereas temperatures peak centuries later (2250–2500) at around 3°C and 9°C, respectively (Fig. 1c). Temperatures then decrease more slowly, remaining elevated by 2°C and 7.5°C by 4000 CE, illustrating strong climate-system inertia.

Despite this persistent warming, several climate components exhibit substantial recovery after peak forcing. Warming-induced sea-ice retreat increases solar absorption and leads to the loss of summer Arctic sea ice within the first few centuries in all scenarios (Fig. 2b). Summer sea ice recovers in the low-emission pathways (SSP2-4.5 and SSP4-6.0), but remains absent for millennia in high-emission scenarios (SSP3-7.0 and SSP5-8.5). Winter sea ice shows smaller losses (approx. 30%) in low-emission scenarios but disappears entirely in high-emission cases, with only partial millennial-scale recovery (Fig. 2a). In the overshoot experiment SSP5-8.5$^*_i$, with a fast reduction of CO_2 forcing, both summer and winter sea ice recover within decades after CO_2 decline, reaching levels comparable to SSP4-6.0$_i$ despite higher air temperatures. These results indicate a general reversibility of Arctic sea-ice loss once CO_2 concentrations decline after an overshoot.

A qualitatively similar behaviour holds for the Atlantic Meridional Overturning Circulation (AMOC) (Fig. 3b). From around 16 Sv in the pre-industrial control simulation, it decreases to around 10 Sv and 5 Sv in SSP2-4.5 and SSP5-8.5, respectively. The AMOC slowdown is dominated by thermal forcing, and its minimum coincides with peak atmospheric CO_2 concentration. Recovery of the AMOC is evident in all simulations. While reaching nearly pre-industrial levels by the year 4000 CE in SSP2-4.5 and SSP4-6.0, it remains weakened at around 13 Sv in SSP3-7.0 and SSP5-8.5. Overshoot behavior occurs in SSP5-8.5$^*_i$ with a fast increase from 10 to 19 Sv. AMOC recovery can be explained by enhanced atmospheric freshwater export from the Atlantic basin under a warmer-than-present climate [32, 46, 47].

Irreversible components: Greenland ice sheet

The Greenland Ice Sheet response is strongly scenario-dependent. High-emission pathways produce several metres of sea-level rise by 4000 CE, around 6 m in SSP3-7.0 and 7.2 m through a complete ice-sheet loss in SSP5-8.5 (Fig. 4a). In low-emission scenarios, projected ice loss corresponds to 1.5 to 3 m of global mean sea-level rise.

The integrated surface mass balance (SMB) is positive during the historical period while being negative at GrIS margins (Fig. A4, A12). Snow accumulation exceeds melting and refreezing further increases SMB. Steeply increasing with temperature, melt rates peak around 2500 CE with maximum global mean temperatures. Integrated meltrates reach 1,500 to 3,500 Gt yr^{-1}, and hence a three- to seven-fold increase from its historical mean (Fig. A3) in SSP4-6.0$_i$ and SSP5-8.5$_i$, respectively. During the 21st century, the SMB becomes negative and dominates ice loss, while calving rates (discharge) decrease from around 300 Gt yr^{-1} to around 100 Gt yr^{-1} in SSP4-6.0$_i$ and become zero when all ocean terminating glaciers have disintegrated (Fig. 4, A4). Basal melting plays only a minor role in the total GrIS mass balance (Fig. A4). By 2100, positive SMB remains only in central west and southeastern Greenland in SSP5-8.5$_i$ (Fig. 4). The ice retreats toward central Greenland, leaving a 2,000 m–thick remnant by 3000 CE and is disintegrated entirely by 4000 CE. In the overshoot experiment SSP5-8.5$^*_i$, the mass balance responds rapidly to reduced forcing and stabilizes at around 1.45 m sea-level equivalent (Fig. 4). In simulations with prescribed GrIS, all precipitation contributes directly to runoff [48], increasing freshwater discharge from around 0.03 Sv under pre-industrial conditions in PI$_i$ to around 0.05 to 0.06 Sv in SSP3-7.0 and SSP5-8.5, with only minor changes in low-emission scenarios (Fig. 3). Including an interactive ice sheet substantially enhances runoff, reaching 0.1 and 0.15 Sv in SSP3-7.0$_i$ and SSP5-8.5$_i$, respectively, and 0.05 to 0.06 Sv in the low-emission cases. Thus, meltwater roughly doubles freshwater input in high-emission scenarios. In the overshoot experiment SSP5-8.5$^*_i$, freshwater release declines rapidly as melting decreases and the ice sheet stabilizes. In our simulations, most of the melting land ice is discharged in the western and northern parts of Greenland. From there, the freshwater is exported out of the North Atlantic region along the Labrador Current. This result underscores the importance of interactive ice-sheet components in future scenario simulations to account for the spatial heterogeneity of meltwater discharge from the ice sheet.

Timescale mechanism: climate memory

The contrasting behavior of different Earth system components reflects differences in intrinsic timescales and feedback processes. Ocean circulation and sea ice respond rapidly to changing radiative forcing and recover once greenhouse gas concentrations decline. In contrast, ice-sheet evolution is governed by slow dynamical and feedback processes, that operate on millennial timescales. In our simulations, peak radiative forcing persists for several centuries, whereas the dynamical adjustment of the GrIS unfolds over millennia. The intrinsic adjustment time of the GrIS therefore exceeds the

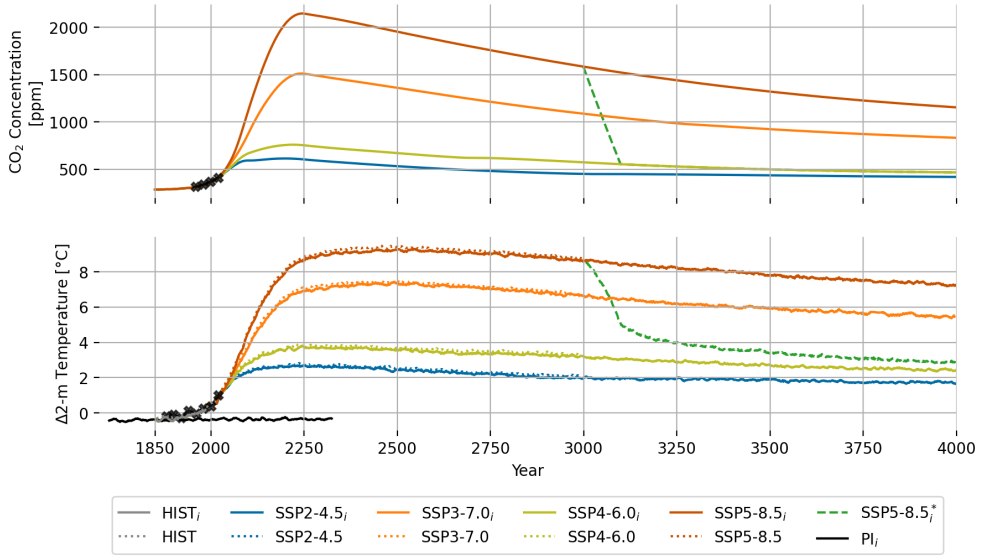

Fig. 1 Time series of atmospheric CO_2 concentrations (a), and global mean air temperature anomalies compared to the mean between 1951 and 1980 (b) for historical (HIST) and different future scenarios (SSP) simulations, as well as a pre-industrial control (PI_i) simulation with a constant 1850 CO_2 concentration. The index i indicates simulations with the interactive Greenland ice sheet. HIST simulations go from 1850 to 2015, and SSP simulations without interactive ice sheet go from 2016 to 3000 CE, while simulations with interactive ice sheet go from 2016 to 4000 CE. SSP5-8.5$_i^*$ is branched off from SSP5-8.5$_i$ in 3000 CE with atmospheric CO_2 concentration linearly decreasing to SSP4-6.0 values within one century. The black crosses in (a) represent observational data from [49] while the black crosses in (b) represent observational data from [44, 45].

duration of peak forcing substantially. This separation of timescales explains why transient overshoot warming results in long-term commitment despite declining greenhouse gas concentrations.

A notable difference between model runs with interactive ice sheet and those without is the reduced summer sea-ice cover and the delayed recovery of both summer and winter sea-ice. A multi-centennial delay in sea-ice recovery occurs for winter sea-ice in SSP3-7.0$_i$, and for summer sea-ice in SSP2-4.5$_i$ and SSP4-6.0$_i$ (Fig. 2b). Increased near-surface air temperatures, driven by ice-albedo and ice-elevation feedback, especially in northern Greenland, lead to this delayed response (Fig. A1, A2). A critical link between potential Earth system tipping elements that is neglected in simulations without an interactive ice sheet.

Differences in AMOC trajectories between simulations with and without an interactive ice sheet are small compared to scenario differences, although the influence of Greenland meltwater on the AMOC increases with GrIS melt rates (Fig. 3). In SSP5-8.5$_i$, GrIS melting adds 0.1 Sv of freshwater and weakens the AMOC by around 1 Sv compared to SSP5-8.5. The additional weakening arises from reduced deep convection in the Labrador and Irminger Seas in SSP5-8.5$_i$ relative to SSP5-8.5 (Fig. 3, A14). However, our results show a comparably weak AMOC sensitivity to Greenland ice

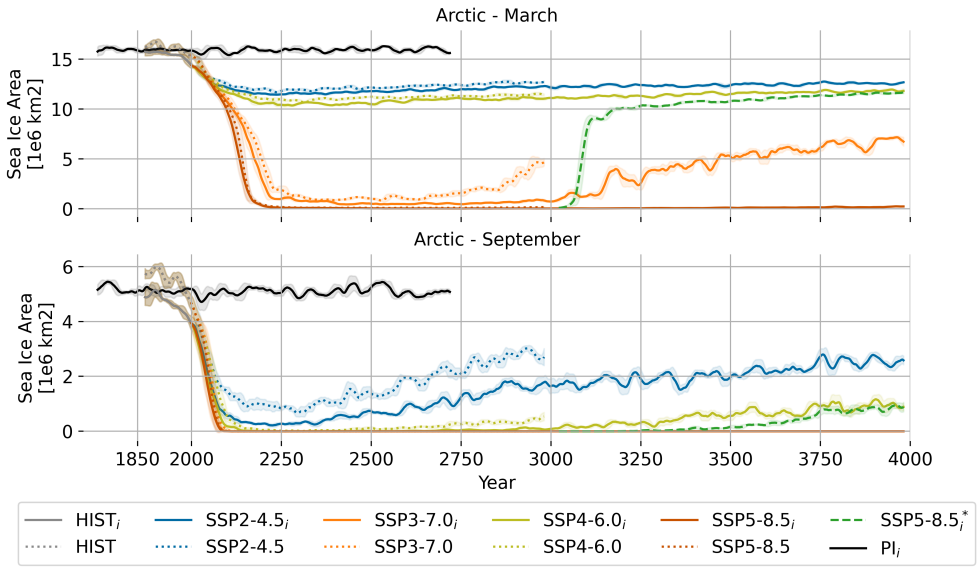

Fig. 2 Time series for Arctic sea ice cover during March (a) and September (b) for historical (HIST) and different future scenarios (SSP) with ("$_i$") and without interactive ice sheet, as well as the control simulation (PI$_i$) (see Fig. A1,A2).

melting, reflecting the spatial pattern of freshwater release and its advection (Fig. 3). As shown in other studies, AMOC response depends strongly on the location of freshwater input [12, 13]. In our simulations, freshwater released mainly north and west of Greenland is transported southward by the East Greenland, West Greenland, and Labrador Currents, producing only limited freshening in the Nordic and Labrador Seas despite large local fluxes in SSP5-8.5$_i$ (Figs. 3, A5, A6). Although only small, the difference in AMOC response due to enhanced GrIS melting dampens warming over the North Atlantic by around 1°C (Fig. A11) through a reduced northward heat transport.

These results show that reversibility in the Earth system is controlled by the interaction between forcing duration and intrinsic process timescales. Components with short adjustment times recover after overshoot warming, whereas slow components, such as ice sheets, store a long-term climate memory and remain committed to change. A nuanced interplay exists in which slow-responding components modulate the trajectories of fast-responding ones.

Discussions

We explore millennial-scale Earth system trajectories under four future warming scenarios using AWI-ESM including an interactive Greenland Ice Sheet. The simulations enable an assessment of transient dynamics and long-term recovery potential.

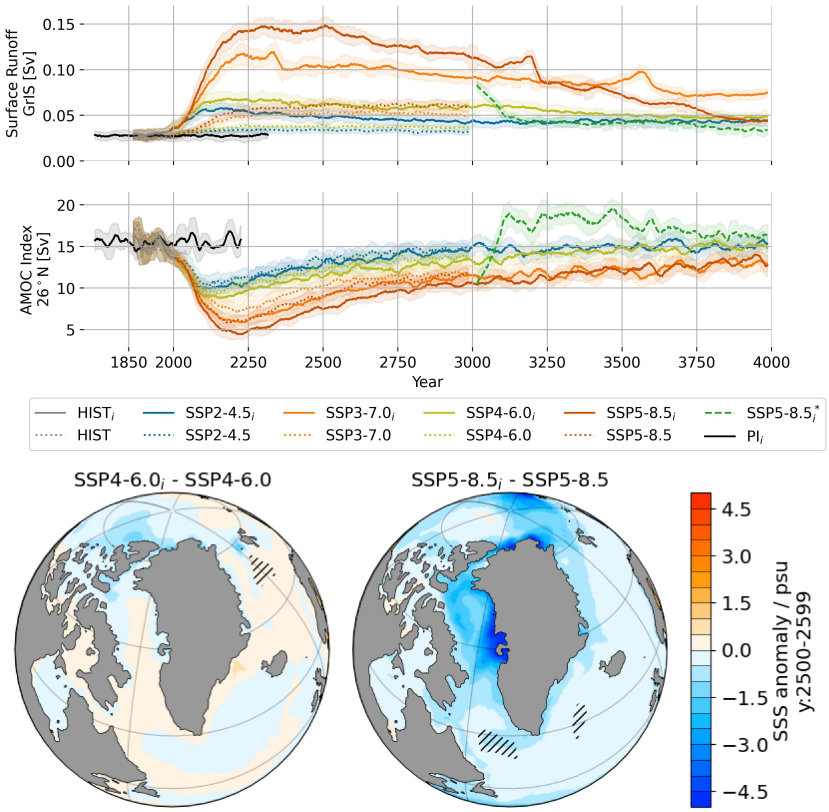

Fig. 3 Timeseries for a) meltwater discharge from Greenland; b) AMOC index as maximum at 26°N for historical (HIST) and future scenarios (SSP), as well as the pre-industrial control run (PI$_i$); c) difference of sea surface salinity between SSP4-6.0$_i$ and SSP4-6.0 averaged between 2500 CE to 2599 CE; d) same as c) but for SSP5-8.5$_i$ and SSP5-8.5. Shaded areas indicate regions where DJF mixed layer depth is reduced by more than 200 m in simulations with interactive GrIS (SSP4-6.0$_i$ and SSP5-8.5$_i$) compared to those without (SSP4-6.0 and SSP5-8.5, see Fig. A14).

The contrasting behaviour of individual climate components in our simulations can be interpreted through a framework of timescale competition. We define timescale competition as the interaction between the duration of external radiative forcing and the intrinsic adjustment timescale of a given Earth system component. When the latter one is short relative to the duration of peak forcing, the component follows the forcing trajectory and may recover once greenhouse gas concentrations decline. In contrast, when intrinsic adjustment times substantially exceed peak forcing duration, the subsystem integrates the perturbation over extended periods and remains committed to long-term change even after atmospheric forcing decreases. In our simulations, Arctic sea-ice and the AMOC are comparatively fast components, adjusting within centuries and recovering once radiative forcing weakens. The GrIS, by contrast, exhibits multi-millennial adjustment times governed by ice dynamics and geometry-dependent feedback, like ice-albedo and ice-elevation feedback. As a consequence, even transient

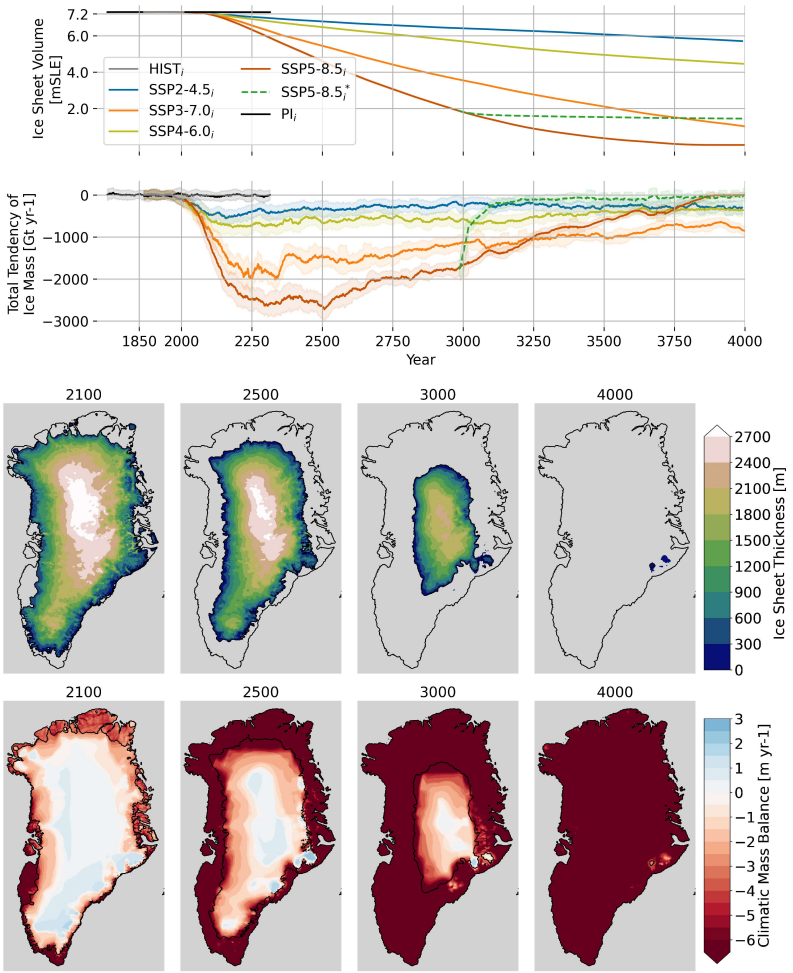

Fig. 4 Timeseries of GrIS a) volume expressed as potential global mean sea level rise, and b) total mass balance for historical (HIST$_i$) and future scenarios (SSP), as well as the pre-industrial control run (PI$_i$); c-f) ice sheet thickness for time slices 2100 CE, 2500 CE, 3000 CE, 4000 CE in the SSP5-8.5$_i$ run; g-j) annual surface mass balance for same time slices as c-f).

overshoot warming leads to persistent mass loss and long-term commitment. This separation of intrinsic timescales implies that tipping behaviour is not determined solely by temperature thresholds, but by the relative magnitude of forcing duration and subsystem adjustment time. Overshoot therefore reorganizes the hierarchy of tipping elements according to their dynamical inertia. In our simulations, the duration of peak forcing is on the order of centuries, whereas GrIS adjustment unfolds over millennia.

Through this long-term memory effect, slow Earth system components shape future climate trajectories. A nuanced interplay between heterogeneous ice-sheet melting, ocean circulation, and deep convection modulates the AMOC response to climate forcing. Instead of a total shutdown, the AMOC recovers even with substantial freshwater

input from GrIS melting, challenging previous studies that project a collapse under sustained warming [22, 41]. However, the somewhat weaker AMOC dampens North Atlantic warming, leading to a regional-scale climate response towards the long-term committed ice sheet. By feedback processes, the GrIS modulates and delays the Arctic sea-ice response on a multi-centennial timescale, even in moderate emission scenarios.

Our results reflect a hierarchy of response times, giving the Earth system a physical memory that extends beyond peak warming. Hence, a comprehensive understanding of system inertia and feedback is essential for informed climate risk management in the Anthropocene. Overall, our results emphasize that early and sustained reductions in carbon emissions not only reduce near-term impacts but also lower the risk of long-term consequences, even if Earth system changes remain potentially reversible. The Earth system's capacity for eventual stabilization should not be misinterpreted as resilience of environmental or social systems, many of which may not withstand such prolonged disruptions.

Methods

CLIMBER-X

The fast Earth system model CLIMBER-X [50, 51] is used to derive the atmospheric CO_2 and CH_4 concentrations needed to force the AWI-ESM. The interactive carbon cycle in the model allows to prognostically simulate the evolution of atmospheric CO_2 and CH_4 given their anthropogenic emissions for the different scenarios. Further details can be found in [52].

AWI-ESM-2

The Alfred Wegener Institute Earth System Model (AWI-ESM) is a comprehensive Earth system model based on the AWI Climate Model (AWI-CM), which has been extensively applied in both paleoclimate and future climate simulations and contributed to the Coupled Model Intercomparison Project Phase 6 (CMIP6) [32, 53–57]. The model version used in this study includes an updated version of the Finite volumE Sea ice–Ocean Model (FESOM2) [56, 58, 59]. FESOM2 employs an unstructured mesh, which has been widely used in past, present, and future climate applications [32, 60, 61], and enables variable horizontal resolution: up to 20 km in high-latitude regions and up to 120 km in lower latitudes, with 47 vertical levels. The atmospheric component of AWI-ESM-2 is ECHAM6, the sixth-generation general circulation model developed by the European Centre for Medium-Range Weather Forecasts [62]. In this study, it is run in the T63L47 configuration, corresponding to a horizontal resolution of approximately 1.9° and 47 vertical levels. ECHAM6 includes a hydrological discharge scheme for simulating river runoff [48] and a dynamic land surface model that represents vegetation processes [63, 64]. The Greenland ice sheet is modelled with the Parallel Ice Sheet Model (PISM) [65, 66]. The model employs the shallow shelf and shallow ice approximations and runs on a local equidistant grid with 5 km horizontal resolution and 201 vertical levels. The surface mass balance for

the ice sheet is calculated by the diurnal Energy Balance Model (dEBM) [67]. This one-dimensional energy balance model receives downscaled precipitation, temperature, shortwave and longwave radiation, and cloud cover fields, and provides the GrIS surface mass balance on the ice-sheet grid. It provides fields for snow accumulation, melting, and refreezing, which sum to the surface mass balance (Fig. A3). The fields are bilinearly interpolated from the atmosphere to the ice-sheet grid, and a lapse-rate correction of 0.005 K m^{-1} is applied.

Experiment design

The multi-millennial future simulations with extended greenhouse gas forcing and prescribed orbital forcing are performed with AWI-ESM. Four different Shared Socioeconomic Pathway (SSP) scenarios are run with ("$_i$") and without interactive Greenland ice sheet (SSP2-4.5, SSP3-7.0, SSP4-6.0, and SSP5-8.5). Atmospheric CO_2 and CH_4 concentrations are prescribed and extended to the year 4000 CE (Fig. 1). The fast Earth system model CLIMBER-X is used to obtain atmospheric CO_2 and CH_4 concentrations from emission-driven scenarios [7, 68]. Orbital parameters are derived after [69]. One additional experiment is performed (SSP5-8.5$^*_i$), which is branched off from SSP5-8.5$_i$, but CO_2 and CH_4 concentrations are linearly reduced to SSP4-6.0$_i$ values between 3000 CE and 3100 CE.

The spinup procedure is as follows: first, the climate model (AWI-ESM) was spun up in a standalone fashion for 1,500 years. Then, AWI-ESM was coupled to PISM and run for two 30-year iterations with back-and-forth coupling between the climate and the ice sheet to obtain a climatological surface mass balance for the ice sheet and an updated orography for the atmosphere model component. Initial ice sheet thickness and bedrock topography are taken from BEDMAP [70] (Fig. A7). A PISM standalone spinup is run with the climatological SMB for 50,000 years. Then, AWI-ESM and PISM are run together asynchronously coupled for 120 (AWI-ESM) and 600 (PISM) years, respectively. The model is then run synchronously coupled for another 130 years, from which the historical simulation (HIST$_i$) branches off.

While few models include a fully interactive Antarctic ice sheet (AIS) [26, 27, 71], its implementation remains challenging for future projections due to the changing land-sea mask and ice shelf geometry. We therefore only account for an interactive GrIS and prescribe the AIS.

Validation

Model results are validated against observational data and multi-model ensemble results. Simulated historical atmospheric CO_2 concentrations match well with observations from [49] (Fig. 1b); modelled historical global mean temperature increase matches well with observations from [44, 45] (Fig. 1c); modelled historical GrIS SMB components are largely within the uncertainty range of [72] (Fig. A8); and SSP5-8.5$_i$ GrIS volume and SMB change match well with ISMIP6 results for the corresponding CMIP5 emission scenario RCP8.5 [73] (Fig. A9). While our results do not allow

for a comprehensive stability analysis of the Greenland ice sheet, a recovery beyond 4000 CE seems unlikely as all scenarios show a global mean temperature increase well above the critical threshold of 1.6°C as assumed by other studies [8–10, 74]. However, duration and magnitude of the temperature overshoot matter, and stable intermediate states might exist for the GrIS [8, 75].

Acknowledgements. Thanks go to the Max Planck Institute in Hamburg (Germany) and colleagues from the Alfred Wegener Institute (AWI) for making ECHAM6-JSBACH and FESOM available to us. The simulations presented in this study are performed using the esm_tools [76]. Model simulations were performed on the high-performance computer "Levante" of the German Climate Computing Center (Deutsches Klimarechenzentrum, DKRZ). For the post-processing and plotting of FESOM data, the Python package "tripyview" (https://github.com/FESOM/tripyview) was used. The work was supported by the research topic "Ocean and Cryosphere under climate change" in the program "Changing Earth – Sustaining our future" of the Helmholtz Society.

Funding

Open access funding provided by Alfred-Wegener-Institut. L.A. acknowledges funding from the Federal Ministry for Education and Research initiative PalMod (grant no. 01LP2313A to G.K. and G.L.). G.L. and G.K. are supported by the ERC synergy grant 'i2B' (grant no. 101118519). The work is also supported by BMBF through the Programme 'Changing Earth-Sustaining our Future' and the Helmholtz Climate Initiative REKLIM (Regional Climate Change), a joint research project of the Helmholtz Association of German research centres (HGF). C.R. has received funding from the European Union's Horizon 2020 research and innovation programme under grant agreement 869304 (PROTECT project) and grant agreement 101184962 (LIQUIDICE). The research of Y.S. was supported by Federal Ministry of Research, Technology and Space (BMFTR) as Research for Sustainability initiative (FONA) through the PalMod project (FKZ: 01LP2309A). MW is funded by the German climate modelling project PalMod supported by the German Federal Ministry of Education and Research (BMBF) as a Research for Sustainability initiative (FONA) (grant no. 01LP2305B)

Conflict of interest

The authors declare no conflict of interest.

Data availability

The CLIMBER-X model data used as forcing for AWI-ESM are available via Zenodo at https://zenodo.org/records/18715605. The AWI-ESM model data discussed in this study are available via Zenodo at https://doi.org/10.5281/zenodo.18718689. The initial ice sheet topography, historical CO_2 and temperature data, and data used for validation are available from the referenced sources.

Code availability

The AWI Earth System Model (AWI-ESM, version 2.1) consists of the atmospheric component ECHAM6 (including land surface scheme JSBACH) and the ocean–sea ice component FESOM (https://fesom.de/models/awi-esm/). The ECHAM6 model is distributed by the Max Planck Institute for Meteorology in Hamburg and is available upon request. A modified version can be found at https://gitlab.awi.de/paleodyn/Models/echam6. Registration at https://code.mpimet.mpg.de/projects/mpi-esm-license is required prior to use of ECHAM6. The Parallel Ice Sheet Model PISM is available via Github at https://github.com/pism/pism. The coupling between the climate model and the ice sheet model is done via ESM-Tools from Github at https://github.com/esm-tools/esm_tools. The energy balance model dEBM is available at https://github.com/ukrebska/dEBM.

Author contribution

MW performed simulations with the CLIMBER-X model. LA performed simulations with the AWI-ESM. UKK, YS, and CR helped with the model setup for AWI-ESM. LA, GK, and GL wrote the first draft. LA, MW, GK, and GL contributed to the interpretation and discussion of the results. All authors provided input to the final version of the manuscript.

Corresponding author

Correspondence to Lars Ackermann

Editorial Policies for:

Springer journals and proceedings: https://www.springer.com/gp/editorial-policies

Nature Portfolio journals: https://www.nature.com/nature-research/editorial-policies

Scientific Reports: https://www.nature.com/srep/journal-policies/editorial-policies

BMC journals: https://www.biomedcentral.com/getpublished/editorial-policies

Appendix A Extended data

Table A1 Summary of simulations run in this study

experiment ID	scenario	interac. ice	length [years]
SSP2-4.5	SSP2-4.5	no	1,150
SSP3-7.0	SSP3-7.0	no	1,150
SSP4-6.0	SSP4-6.0	no	1,150
SSP5-8.5	SSP5-8.5	no	1,150
SSP2-4.5$_i$	SSP2-4.5	yes	2,150
SSP3-7.0$_i$	SSP3-7.0	yes	2,150
SSP4-6.0$_i$	SSP4-6.0	yes	2,150
SSP5-8.5$_i$	SSP5-8.5	yes	2,150
PI$_i$	1850[1]	yes	800
SSP5-8.5$^*_i$	3000	yes	1000

[1]The PI$_i$ simulation is run with fixed greenhouse gas and orbital forcing for the year 1850.

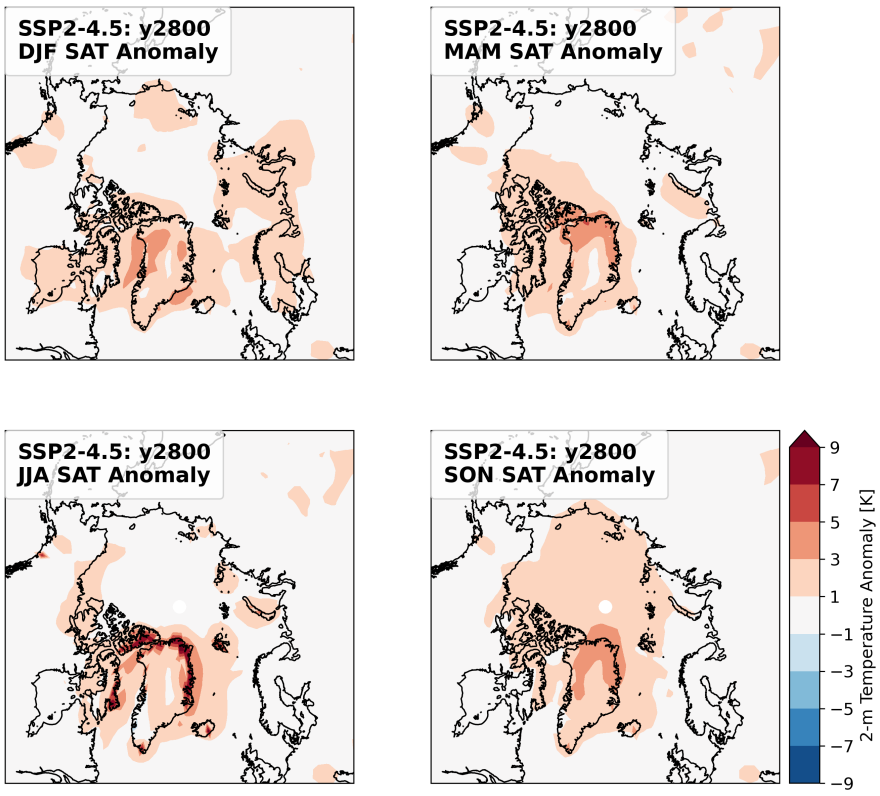

Fig. A1 Seasonal atmospheric 2-m temperature difference between SSP2-4.5$_i$ and SSP2-4.5 averaged between 2800 CE and 2849 CE.

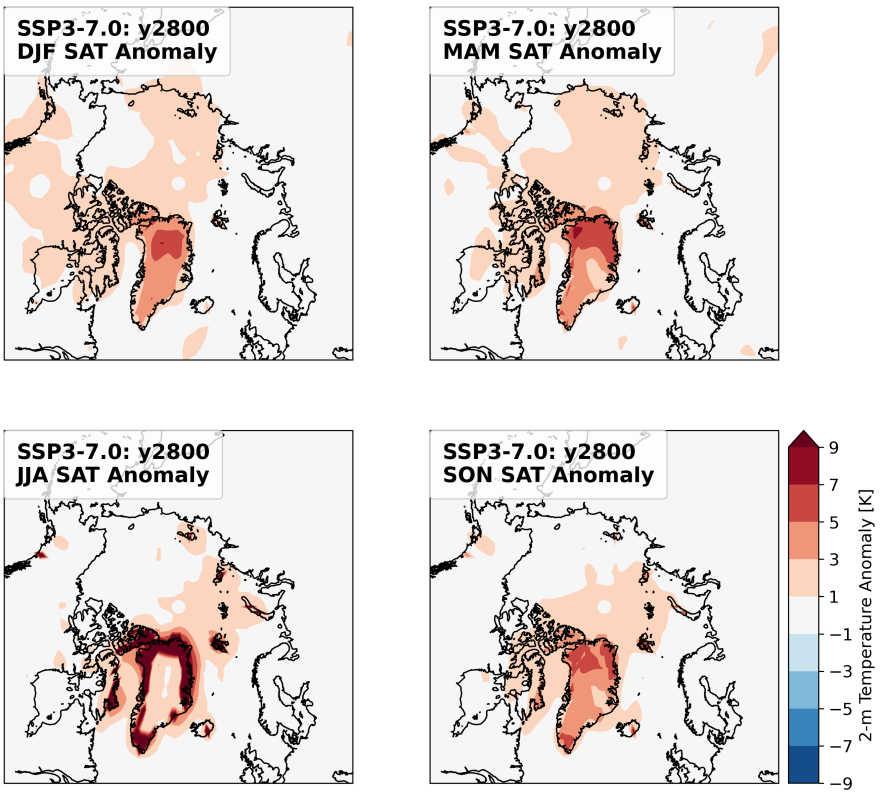

Fig. A2 Seasonal atmospheric 2-m temperature difference between SSP3-7.0$_i$ and SSP3-7.0 averaged between 2800 CE and 2849 CE.

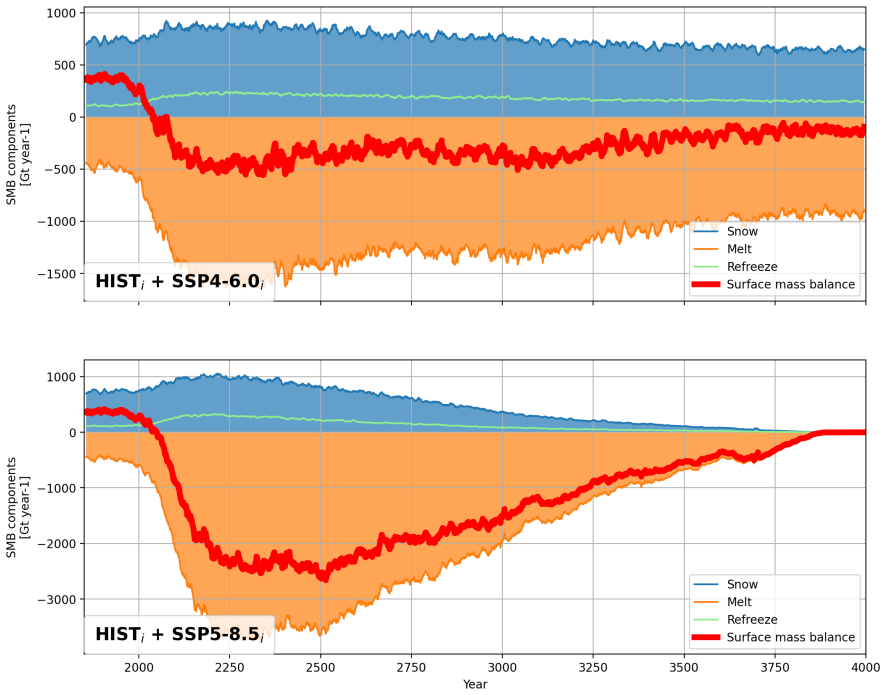

Fig. A3 Timeseries of GrIS surface mass balance components accumulation (snow), melting, and refreezing for a) SSP4-6.0$_i$ and b) SSP5-8.5$_i$.

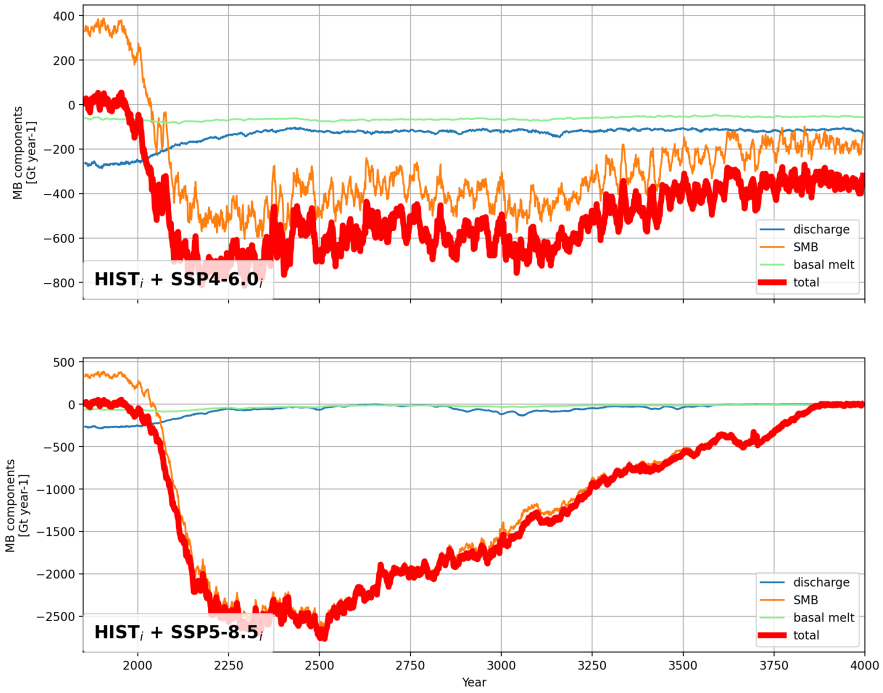

Fig. A4 Timeseries of GrIS mass balance components calving (discharge), surface mass balance (SMB), and basal melting for a) SSP4-6.0$_i$ and b) SSP5-8.5$_i$.

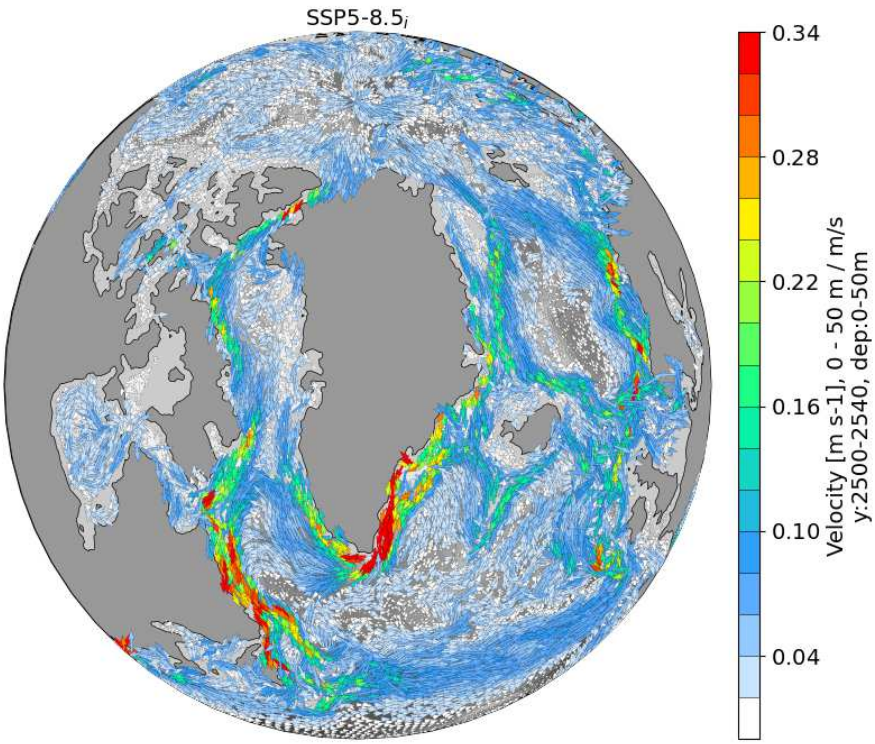

Fig. A5 Horizontal velocities in the North Atlantic averaged between 2500 CE and 2549 CE for SSP5-8.5$_i$.

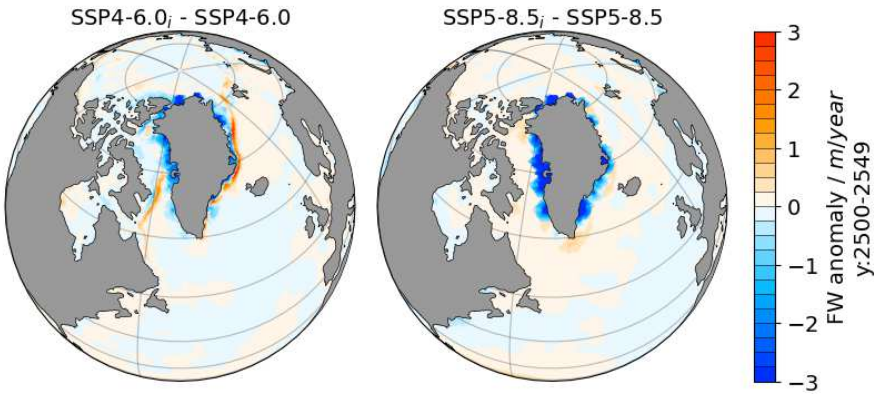

Fig. A6 a) Difference of surface freshwater fluxes between SSP4-6.0$_i$ and SSP4-6.0 averaged between 2500 CE and 2549 CE; b) same as a) but for SSP5-8.5$_i$ and SSP5-8.5.

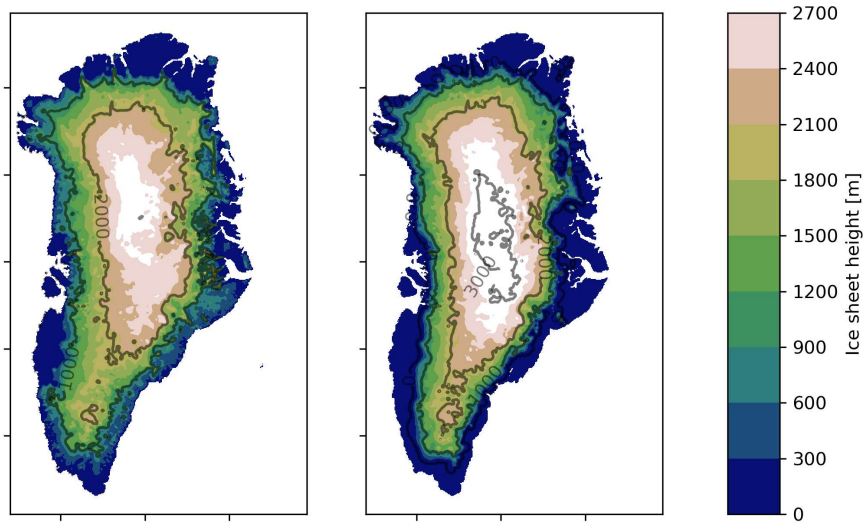

Fig. A7 a) Initial ice sheet thickness used for HIST$_i$; b) ice sheet thickness from BEDMAP [70].

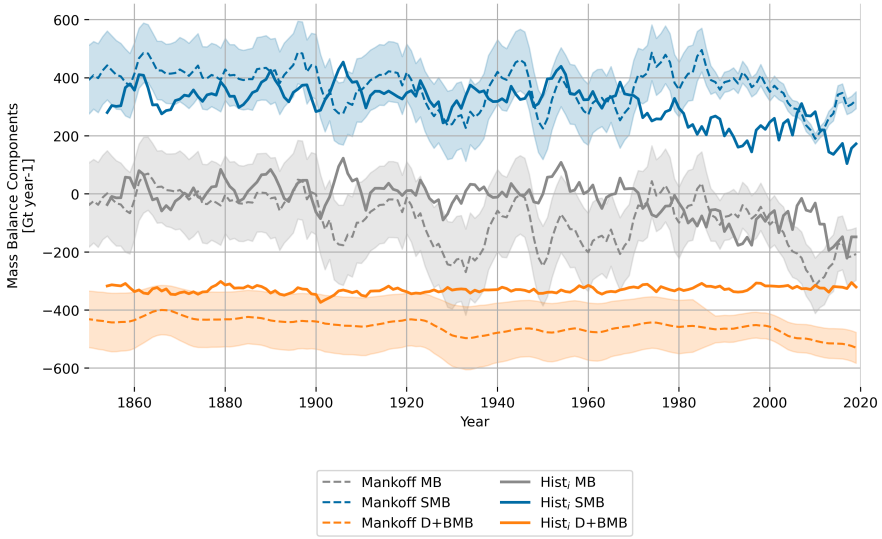

Fig. A8 Timeseries of different Greenland ice sheet mass balance components for HIST$_i$ compared to different regional models from [72]. Shaded areas indicate model uncertainty.

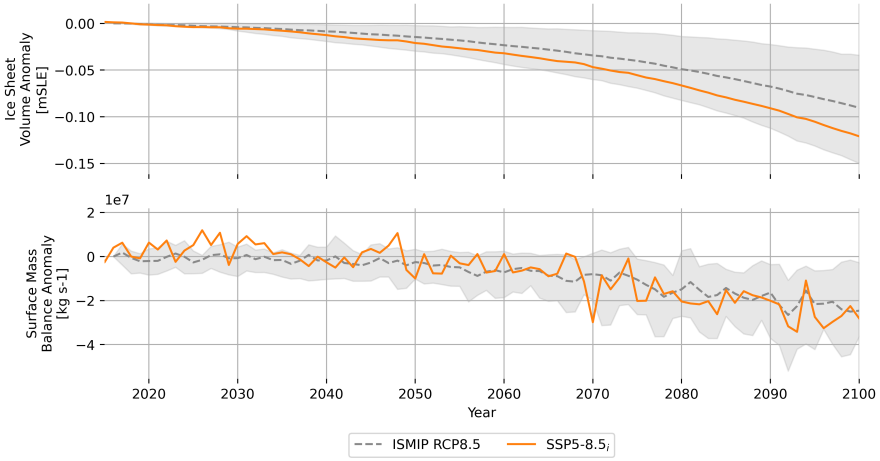

Fig. A9 Timeseries for a) Greenland ice volume anomaly expressed as potential global mean sea level rise, and b) surface mass balance anomaly with respect to 2018 for SSP5-8.5$_i$ compared to the RCP8.5 scenario simulations done for ISMIP6 [73]. Shaded areas indicate multi-model spread.

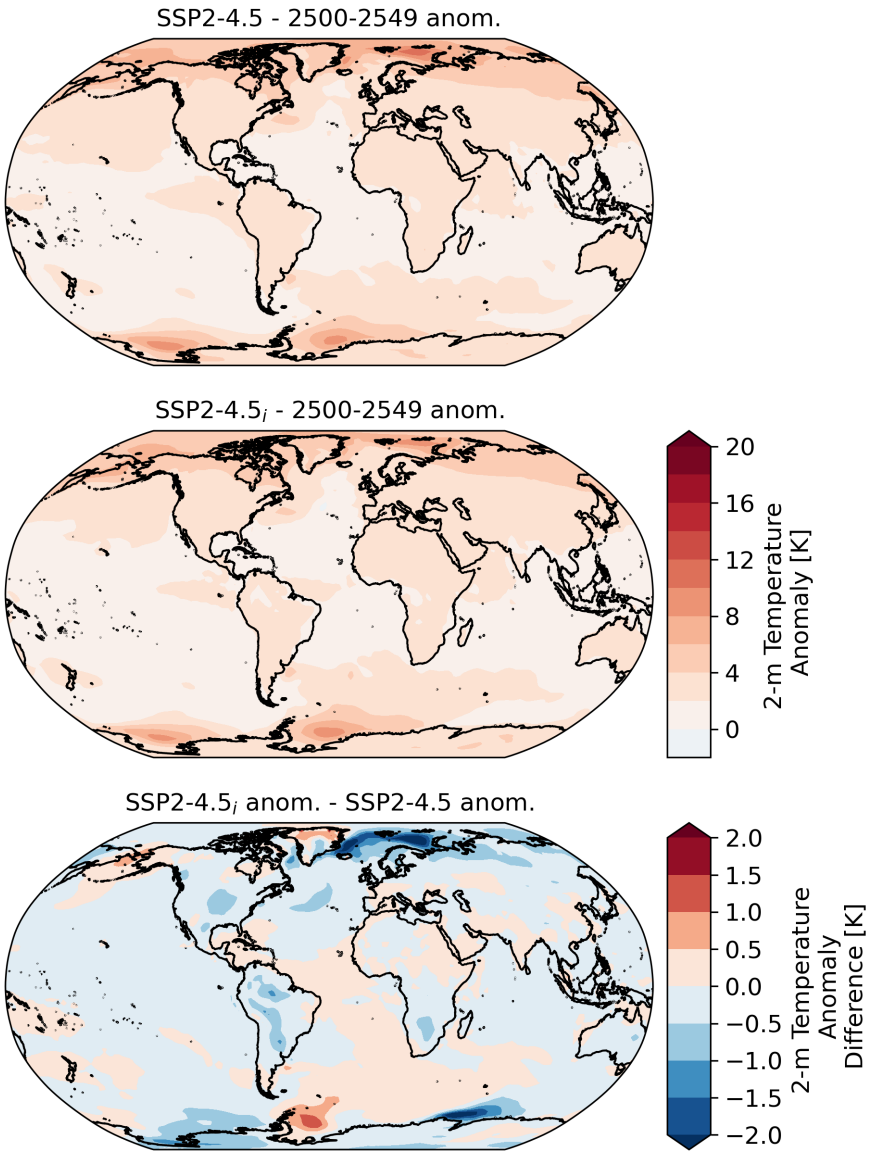

Fig. A10 Atmospheric 2-m temperature difference between SSP2-4.5$_i$ and SSP2-4.5 averaged between 2500 CE and 2549 CE.

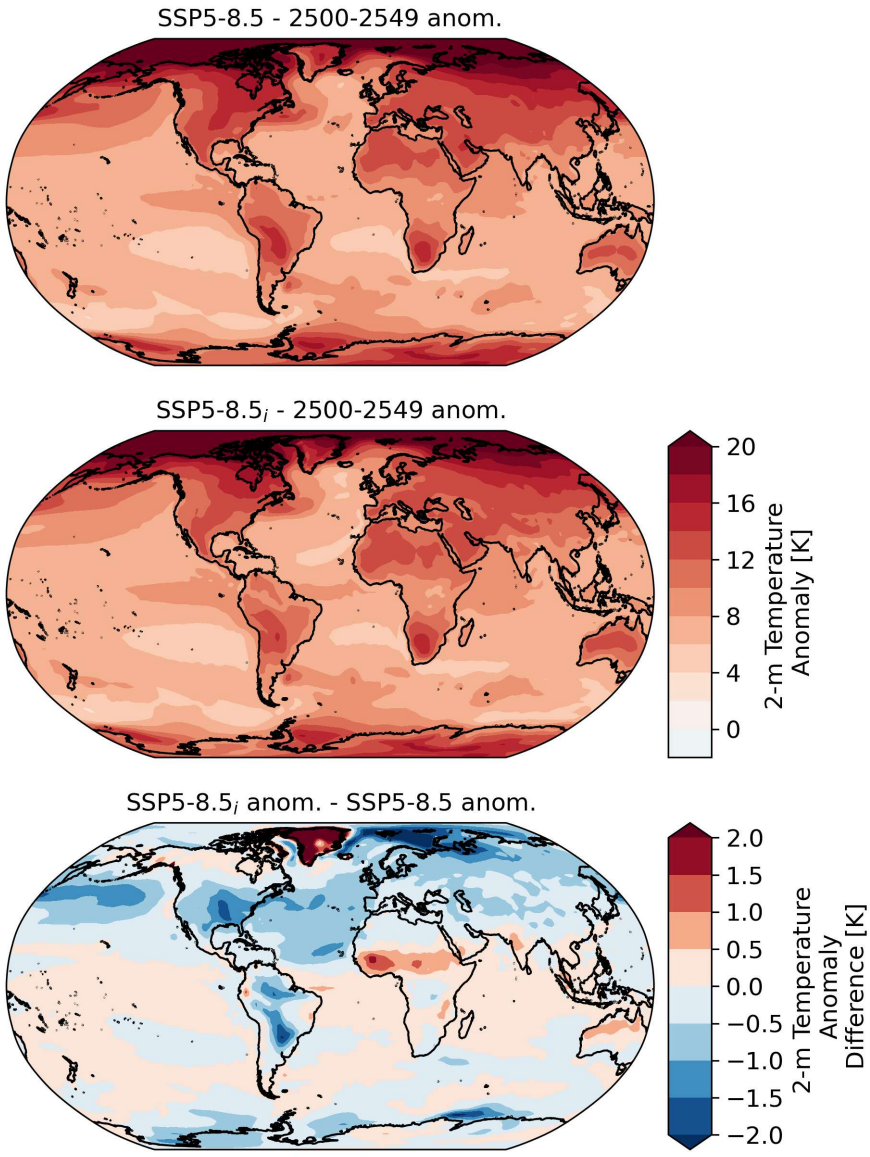

Fig. A11 Atmospheric 2-m temperature difference between SSP3-7.0$_i$ and SSP3-7.0 averaged between 2500 CE and 2549 CE.

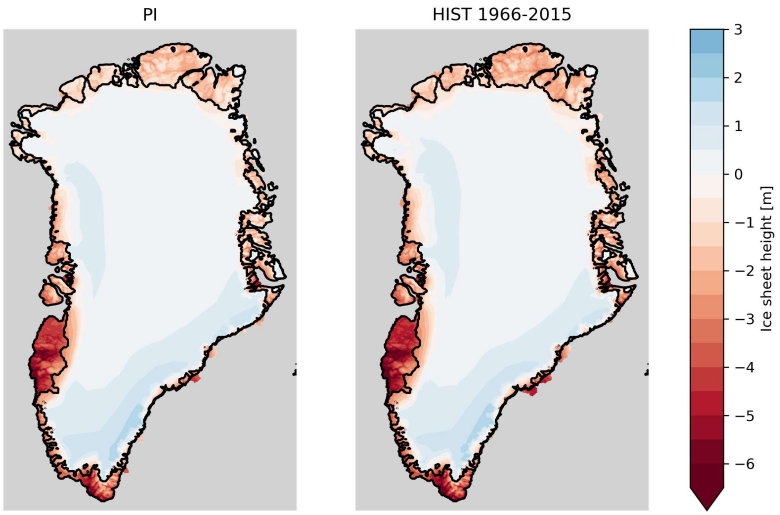

Fig. A12 Initial ice sheet thickness and reference topography from [70].

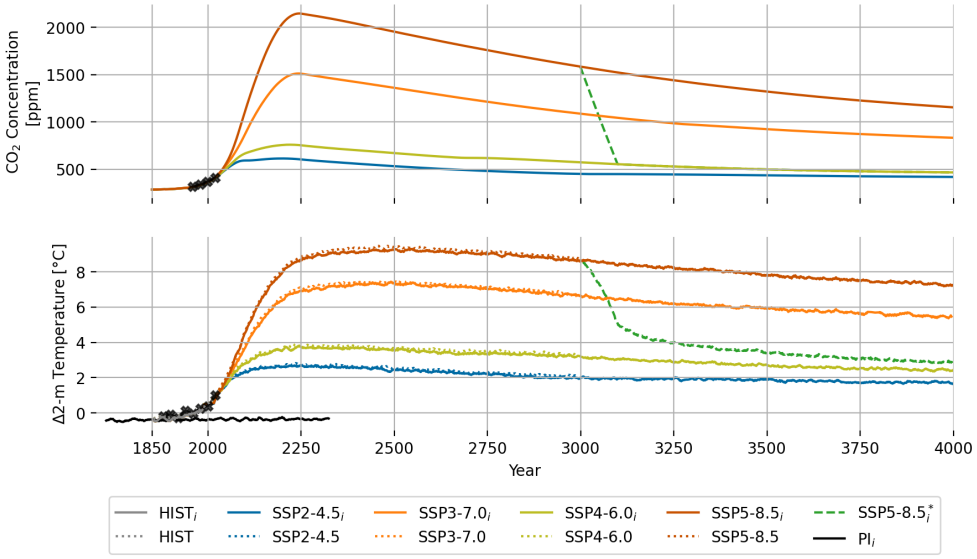

Fig. A13 Time series of CO_2 emissions (a), atmospheric CO_2 concentrations (b), and global mean air temperature anomalies compared to the mean between 1951 and 1980 (c) for historical (HIST) and different future scenarios (SSP) simulations, as well as a pre-industrial control (PI_i) simulation with a constant 1850 CO_2 concentration. The index i indicates simulations with the interactive Greenland ice sheet. HIST simulations go from 1850 to 2015, and SSP simulations without interactive ice sheet go from 2016 to 3000 CE, while simulations with interactive ice sheet go from 2016 to 4000 CE. SSP5-8.5$_i^*$ is branched off from SSP5-8.5$_i$ in 3000 CE with atmospheric CO_2 concentration linearly decreasing to SSP4-6.0 values within one century. The black crosses in (b) represent observational data from [49] while the black crosses in (c) represent observational data from [44, 45].

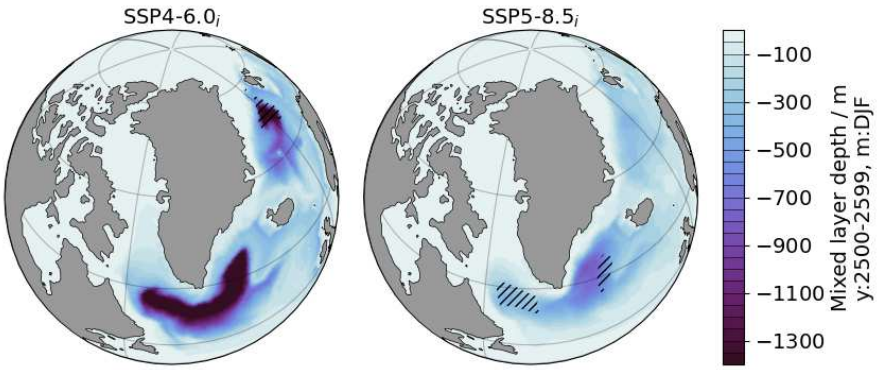

Fig. A14 Mean DJF mixed layer depth for SSP4-6.0$_i$ averaged between 2500 CE and 2599 CE; f) same as e) but for SSP5-8.5$_i$. Shaded areas indicate regions where DJF mixed layer depth is reduced by more than 200 m in simulations with interactive GrIS (SSP4-6.0$_i$ and SSP5-8.5$_i$) compared to those without (SSP4-6.0 and SSP5-8.5).

References

[1] Lenton, T. M. et al. Tipping elements in the earth's climate system. Proceedings of the national Academy of Sciences **105**, 1786–1793 (2008).

[2] Armstrong McKay, D. I. et al. Exceeding 1.5 c global warming could trigger multiple climate tipping points. Science **377**, eabn7950 (2022).

[3] Wunderling, N. et al. Climate tipping point interactions and cascades: A review. Earth System Dynamics **15**, 41–74 (2024).

[4] Solomon, S., Plattner, G.-K., Knutti, R. & Friedlingstein, P. Irreversible climate change due to carbon dioxide emissions. Proceedings of the national academy of sciences **106**, 1704–1709 (2009).

[5] Levermann, A. et al. The multimillennial sea-level commitment of global warming. Proceedings of the National Academy of Sciences **110**, 13745–13750 (2013).

[6] Clark, P. U. et al. Consequences of twenty-first-century policy for multi-millennial climate and sea-level change. Nature climate change **6**, 360–369 (2016).

[7] Meinshausen, M. et al. The shared socio-economic pathway (ssp) greenhouse gas concentrations and their extensions to 2500. Geoscientific Model Development **13**, 3571–3605 (2020).

[8] Robinson, A., Calov, R. & Ganopolski, A. Multistability and critical thresholds of the greenland ice sheet. Nature Climate Change **2**, 429–432 (2012).

[9] Pattyn, F. et al. The greenland and antarctic ice sheets under 1.5 c global warming. Nature climate change **8**, 1053–1061 (2018).

[10] Bochow, N. et al. Overshooting the critical threshold for the greenland ice sheet. Nature **622**, 528–536 (2023).

[11] Stouffer, R. J. et al. Investigating the causes of the response of the thermohaline circulation to past and future climate changes. Journal of climate **19**, 1365–1387 (2006).

[12] Jackson, L. C. et al. Understanding amoc stability: The north atlantic hosing model intercomparison project. Geoscientific Model Development Discussions **2022**, 1–32 (2022).

[13] Ma, Q. et al. Revisiting climate impacts of an amoc slowdown: dependence on freshwater locations in the north atlantic. Science Advances **10**, eadr3243 (2024).

[14] Rockström, J. et al. A safe operating space for humanity. nature **461**, 472–475 (2009).

[15] Steffen, W. et al. Trajectories of the earth system in the anthropocene. Proceedings of the national academy of sciences **115**, 8252–8259 (2018).

[16] Petrini, M. et al. A topographically controlled tipping point for complete greenland ice sheet melt. The Cryosphere **19**, 63–81 (2025).

[17] Screen, J. A. & Simmonds, I. The central role of diminishing sea ice in recent arctic temperature amplification. Nature **464**, 1334–1337 (2010).

[18] Hankel, C. & Tziperman, E. An approach for projecting the timing of abrupt winter arctic sea ice loss. Nonlinear Processes in Geophysics **30**, 299–309 (2023).

[19] Rosser, J. P., Winkelmann, R. & Wunderling, N. Polar ice sheets are decisive contributors to uncertainty in climate tipping projections. Communications Earth & Environment **5**, 702 (2024).

[20] Weijer, W., Cheng, W., Garuba, O. A., Hu, A. & Nadiga, B. T. Cmip6 models predict significant 21st century decline of the atlantic meridional overturning circulation. Geophysical Research Letters **47**, e2019GL086075 (2020).

[21] Baker, J. A. et al. Overturning pathways control amoc weakening in cmip6 models. Geophysical Research Letters **50**, e2023GL103381 (2023).

[22] Drijfhout, S., Angevaare, J. R., Mecking, J., Van Westen, R. M. & Rahmstorf, S. Shutdown of northern atlantic overturning after 2100 following deep mixing collapse in cmip6 projections. Environmental Research Letters **20**, 094062 (2025).

[23] Claussen, M. et al. Earth system models of intermediate complexity: closing the gap in the spectrum of climate system models. Climate dynamics **18**, 579–586 (2002).

[24] Fichefet, T. et al. Implications of changes in freshwater flux from the greenland ice sheet for the climate of the 21st century. Geophysical Research Letters **30** (2003).

[25] Ridley, J. K., Huybrechts, P., Gregory, J. u. & Lowe, J. Elimination of the greenland ice sheet in a high co 2 climate. Journal of Climate **18**, 3409–3427 (2005).

[26] Mikolajewicz, U., Vizcaino, M., Jungclaus, J. & Schurgers, G. Effect of ice sheet interactions in anthropogenic climate change simulations. Geophysical Research Letters **34** (2007).

[27] Vizcaíno, M. et al. Long-term ice sheet–climate interactions under anthropogenic greenhouse forcing simulated with a complex earth system model. Climate dynamics **31**, 665–690 (2008).

[28] Vizcaíno, M., Mikolajewicz, U., Jungclaus, J. & Schurgers, G. Climate modification by future ice sheet changes and consequences for ice sheet mass balance. Climate Dynamics **34**, 301–324 (2010).

[29] Lipscomb, W. H. et al. Implementation and initial evaluation of the glimmer community ice sheet model in the community earth system model. Journal of Climate **26**, 7352–7371 (2013).

[30] Ziemen, F., Rodehacke, C. & Mikolajewicz, U. Coupled ice sheet–climate modeling under glacial and pre-industrial boundary conditions. Climate of the Past **10**, 1817–1836 (2014).

[31] Gierz, P., Lohmann, G. & Wei, W. Response of atlantic overturning to future warming in a coupled atmosphere-ocean-ice sheet model. Geophysical Research Letters **42**, 6811–6818 (2015).

[32] Ackermann, L., Danek, C., Gierz, P. & Lohmann, G. Amoc recovery in a multicentennial scenario using a coupled atmosphere-ocean-ice sheet model. Geophysical Research Letters **47**, e2019GL086810 (2020).

[33] Muntjewerf, L. et al. Description and demonstration of the coupled community earth system model v2–community ice sheet model v2 (cesm2-cism2). Journal of Advances in Modeling Earth Systems **13**, e2020MS002356 (2021).

[34] Kapsch, M.-L., Mikolajewicz, U., Ziemen, F. A., Rodehacke, C. B. & Schannwell, C. Analysis of the surface mass balance for deglacial climate simulations. The Cryosphere **15**, 1131–1156 (2021).

[35] Haubner, K., Goelzer, H. & Born, A. Limited global effect of climate-greenland ice sheet coupling in noresm2 under a high-emission scenario. Earth System Dynamics **17**, 57–80 (2026).

[36] Testorf, P., Schannwell, C., Kapsch, M.-L. & Mikolajewicz, U. Coupled climate-ice-sheet simulations reveal novel teleconnection between northern hemisphere ice sheets and the antarctic ice sheet. Geophysical Research Letters **53**, e2025GL118959 (2026).

[37] Wang, S. et al. Mechanisms and impacts of earth system tipping elements. Reviews of Geophysics **61**, e2021RG000757 (2023).

[38] Yu, L., Gao, Y. & Otterå, O. H. The sensitivity of the atlantic meridional overturning circulation to enhanced freshwater discharge along the entire, eastern and western coast of greenland. Climate Dynamics **46**, 1351–1369 (2016).

[39] Baker, J. et al. Continued atlantic overturning circulation even under climate extremes. Nature **638**, 987–994 (2025).

[40] Lenaerts, J. T. et al. Representing greenland ice sheet freshwater fluxes in climate models. Geophysical Research Letters **42**, 6373–6381 (2015).

[41] Bakker, P. et al. Fate of the atlantic meridional overturning circulation: Strong decline under continued warming and greenland melting. Geophysical Research Letters **43**, 12–252 (2016).

[42] Niu, L., Knorr, G., Krebs-Kanzow, U., Gierz, P. & Lohmann, G. Rapid laurentide ice sheet growth preceding the last glacial maximum due to summer snowfall. Nature Geoscience **17**, 440–449 (2024).

[43] Niu, L., Knorr, G., Ackermann, L., Krebs-Kanzow, U. & Lohmann, G. Eurasian ice sheet formation promoted by weak amoc following mis 3. npj Climate and Atmospheric Science **8**, 85 (2025).

[44] Lenssen, N. et al. A nasa gistempv4 observational uncertainty ensemble. Journal of Geophysical Research: Atmospheres **129**, e2023JD040179 (2024).

[45] Team, G. Giss surface temperature analysis (gistemp), version 4. NASA Goddard Institute for Space Studies (2025).

[46] Latif, M., Roeckner, E., Mikolajewicz, U. & Voss, R. Tropical stabilization of the thermohaline circulation in a greenhouse warming simulation. Journal of Climate **13**, 1809–1813 (2000).

[47] Lohmann, G. Atmospheric and oceanic freshwater transport during weak atlantic overturning circulation. Tellus A: Dynamic Meteorology and Oceanography **55**, 438–449 (2003).

[48] Hagemann, S. & Dümenil, L. A parametrization of the lateral waterflow for the global scale. Climate dynamics **14**, 17–31 (1997).

[49] Keeling, C. D. et al. Atmospheric carbon dioxide variations at mauna loa observatory, hawaii. Tellus **28**, 538–551 (1976).

[50] Willeit, M., Ganopolski, A., Robinson, A. & Edwards, N. R. The earth system model climber-x v1. 0. part 1: Climate model description and validation. Geoscientific Model Development Discussions **2022**, 1–69 (2022).

[51] Willeit, M. et al. The earth system model climber-x v1. 0–part 2: The global carbon cycle. Geoscientific Model Development **16**, 3501–3534 (2023).

[52] Kaufhold, C., Willeit, M., Talento, S., Ganopolski, A. & Rockström, J. Interplay between climate and carbon cycle feedbacks could substantially enhance future warming. Environmental Research Letters **20**, 044027 (2025).

[53] Sidorenko, D. et al. Towards multi-resolution global climate modeling with echam6–fesom. part i: model formulation and mean climate. Climate Dynamics

505 **44**, 757–780 (2015).

506 [54] Rackow, T. et al. Towards multi-resolution global climate modeling with echam6-
507 fesom. part ii: climate variability. Climate Dynamics **50**, 2369–2394 (2018).

508 [55] Semmler, T. et al. Simulations for cmip6 with the awi climate model awi-cm-1-1.
509 Journal of Advances in Modeling Earth Systems **12**, e2019MS002009 (2020).

510 [56] Sidorenko, D. et al. Evaluation of fesom2. 0 coupled to echam6. 3: preindustrial
511 and highresmip simulations. Journal of Advances in Modeling Earth Systems **11**,
512 3794–3815 (2019).

513 [57] Shi, X. et al. Calendar effects on surface air temperature and precipitation
514 based on model-ensemble equilibrium and transient simulations from pmip4 and
515 pacmedy. Climate of the Past **18**, 1047–1070 (2022).

516 [58] Danilov, S., Sidorenko, D., Wang, Q. & Jung, T. The finite-volume sea ice–ocean
517 model (fesom2). Geoscientific Model Development **10**, 765–789 (2017).

518 [59] Scholz, P. et al. Assessment of the finite-volume sea ice-ocean model (fesom2.
519 0)–part 1: Description of selected key model elements and comparison to its
520 predecessor version. Geoscientific Model Development **12**, 4875–4899 (2019).

521 [60] Danabasoglu, G. et al. North atlantic simulations in coordinated ocean-ice ref-
522 erence experiments phase ii (core-ii). part i: mean states. Ocean Modelling **73**,
523 76–107 (2014).

524 [61] Sein, D. V. et al. Designing variable ocean model resolution based on the observed
525 ocean variability. Journal of Advances in Modeling Earth Systems **8**, 904–916
526 (2016).

527 [62] Stevens, B. et al. Atmospheric component of the mpi-m earth system model:
528 Echam6. Journal of Advances in Modeling Earth Systems **5**, 146–172 (2013).

529 [63] Reick, C., Raddatz, T., Brovkin, V. & Gayler, V. Representa-
530 tion of natural and anthropogenic land cover change in mpi-esm.
531 Journal of Advances in Modeling Earth Systems **5**, 459–482 (2013).

532 [64] Reick, C. H. et al. Jsbach 3-the land component of the mpi earth system model:
533 documentation of version 3.2 (2021).

534 [65] Winkelmann, R. et al. The potsdam parallel ice sheet model (pism-pik)–part 1:
535 Model description. The Cryosphere **5**, 715–726 (2011).

536 [66] Martin, M. A. et al. The potsdam parallel ice sheet model (pism-pik)–part 2:
537 dynamic equilibrium simulation of the antarctic ice sheet. The Cryosphere **5**,
538 727–740 (2011).

[67] Krebs-Kanzow, U. et al. The diurnal energy balance model (debm): a convenient surface mass balance solution for ice sheets in earth system modeling. The Cryosphere **15**, 2295–2313 (2021).

[68] Riahi, K. et al. The shared socioeconomic pathways and their energy, land use, and greenhouse gas emissions implications: An overview. Global environmental change **42**, 153–168 (2017).

[69] Berger, A. Long-term variations of daily insolation and quaternary climatic changes. Journal of Atmospheric Sciences **35**, 2362–2367 (1978).

[70] Bamber, J. L., Layberry, R. L. & Gogineni, S. A new ice thickness and bed data set for the greenland ice sheet: 1. measurement, data reduction, and errors. Journal of Geophysical Research: Atmospheres **106**, 33773–33780 (2001).

[71] Smith, R. S. et al. Coupling the uk earth system model to dynamic models of the greenland and antarctic ice sheets. Journal of Advances in Modeling Earth Systems **13**, e2021MS002520 (2021).

[72] Mankoff, K. D. et al. Greenland ice sheet mass balance from 1840 through next week. Earth System Science Data **13**, 5001–5025 (2021).

[73] Goelzer, H. et al. The future sea-level contribution of the greenland ice sheet: a multi-model ensemble study of ismip6. The Cryosphere **14**, 3071–3096 (2020).

[74] Höning, D. et al. Multistability and transient response of the greenland ice sheet to anthropogenic co2 emissions. Geophysical Research Letters **50**, e2022GL101827 (2023).

[75] Andernach, M., Kapsch, M.-L. & Mikolajewicz, U. Stabilizing feedbacks allow for multiple states of the greenland ice sheet in a fully coupled earth system–ice sheet model. The Cryosphere **20**, 1047–1069 (2026).

[76] Barbi, D. et al. Esm-tools version 4.0: A modular infrastructure for stand-alone and coupled earth system modelling (esm). Geoscientific Model Development Discussions **2020**, 1–21 (2020).